

RESEARCH

Open Access



A potential new strategy for BC treatment: NPs containing solanine and evaluation of its anticancer and antimetastatic properties

Nadia Zargarani¹, Mahsa Kavousi^{1*} and Elahe Aliasgari¹

Abstract

Solanine has been shown to inhibit cancer by regulating the expression of apoptosis (*Bax*, *Bcl-2*) and metastasis (*CDH-1*, *MMP2*) genes in various cancer cell types. We synthesized optimized niosome NPs (NPs) with high solubility and capacity for solanine loading. In this study, the cytotoxic, cell cycle inhibitory and apoptotic effects of solanine-loaded niosome NPs (SN-NPs) on MCF-7 were investigated. Thin-layer hydration was used to generate SN-NPs and their features were validated. The pH-dependent solanine release pattern was also examined. Synthesized SN-NPs were evaluated for cytotoxicity against MCF-7 and MCF-10 cell lines using MTT. Primary and secondary apoptosis, necrosis, and cell cycle arrest were measured using flowcytometry. Lastly, q-PCR was used to assess the expression of genes. The NPs had an average size between 50 and 70 nm, with a polydispersity index (PDI) of 0.452. Solanine was effectively incorporated into niosome NPs, as shown by the high encapsulation efficiency of $82.3\% \pm 0.24\%$. After a quick burst at pH 7 and 5, SN-NPs released slowly and sustainedly. The IC_{50} of solanine-loaded niosomes against MCF-7 cells decreased from 40 mg/100 mL to 10 mg/100 mL (48 h) and 5 mg/100 mL (72 h). After 72 h, SN-NPs caused late apoptosis in 30% of MCF-7 cells and necrosis in 5.06% ($p < 0.01$). SN-NPs caused 81% of cells to arrest in the G0/G1 phase, with only 12% progressing to G2/M ($p < 0.01$). Solanine-loaded NPs significantly increased *Bax* and *CDH-1* gene expression in malignant cells compared to free niosomes and free solanine ($p < 0.0001$). *Bcl-2* and *MMP2* expression significantly decreased in this group compared to free niosomes and free solanine ($p < 0.001$). Solanine-containing niosomes showed significant anticancer effects on MCF-7 breast cancer cells, which were supported by apoptosis, cell cycle arrest and regulation of gene expression. The regulated release and precise delivery of solanine using SN-NPs show considerable translational potential. This improved nanocarrier technology may increase the bioavailability and efficacy of solanine, potentially leading to improved clinical outcomes in breast cancer therapy.

Keywords Solanine, NPs, MCF-7, BC, MTT, Flowcytometry

*Correspondence:

Mahsa Kavousi
mkavosi@yahoo.co.uk

¹Department of Biology, East Tehran Branch, Islamic Azad University, Tehran, Iran



© The Author(s) 2025. **Open Access** This article is licensed under a Creative Commons Attribution-NonCommercial-NoDerivatives 4.0 International License, which permits any non-commercial use, sharing, distribution and reproduction in any medium or format, as long as you give appropriate credit to the original author(s) and the source, provide a link to the Creative Commons licence, and indicate if you modified the licensed material. You do not have permission under this licence to share adapted material derived from this article or parts of it. The images or other third party material in this article are included in the article's Creative Commons licence, unless indicated otherwise in a credit line to the material. If material is not included in the article's Creative Commons licence and your intended use is not permitted by statutory regulation or exceeds the permitted use, you will need to obtain permission directly from the copyright holder. To view a copy of this licence, visit <http://creativecommons.org/licenses/by-nc-nd/4.0/>.

Introduction

Breast cancer (BC) is the leading cause of cancer-related deaths in women worldwide, with over 30 million new cases predicted to occur by 2040 [1, 2]. Subtypes such as ER+, PR+, HER2+ and TNBC respond differently to treatment [3, 4]. Surgery, radiation and chemotherapy are conventional therapies; however, recurrence and drug resistance are significant obstacles [5, 6]. Omics studies show heterogeneity within and between tumors, necessitating improved diagnostic and treatment approaches [6, 7].

Nanotechnology enables precise drug delivery, better solubility and lower toxicity than conventional treatments [8, 9]. Nanocarriers, such as niosomes, protect drugs from degradation and thus improve their efficacy. Niosomes are nanoscale vesicles consisting of amphiphilic compounds containing hydrophilic and hydrophobic drugs [10, 11]. Their non-ionic properties provide improved chemical stability and biocompatibility compared to liposomes [12, 13]. Niosomes enable versatile drug loading, controlled release and precise distribution, making them effective drug delivery systems for cancer treatment [14].

The use of natural ingredients in drug development is steadily growing. Throughout many ages, organic substances have been applied to prevent and treat various disorders [15]. A wide range of natural compounds are often used in clinical studies, particularly for their antibacterial and anticancer properties. In recent years, there has been a growing inclination toward using conventional medications and small-molecule anticancer drugs to prevent and treat cancer [16]. Multiple investigations indicate that Gas have the ability to impede the development of many types of cancer cells. Plants naturally synthesize these GAs as defensive poisons to safeguard themselves against adverse conditions, including low temperatures, herbivore grazing, and assaults from plant pathogens [17]. GAs are present in various plants and fruits, with *Solanum tuberosum* being a prominent source of GAs [17]. α -solanine is a trisaccharide glycoalkaloid with the chemical formula $C_{45}H_{73}NO_{15}$. Solanine, a glycoalkaloid present in potatoes and other plants, has restricted water solubility, impeding its therapeutic efficacy. Nevertheless, research has demonstrated its potential anticancer characteristics, notably the capacity to trigger apoptosis in several types of cancer cells [18]. Research indicates that solanine elevated the apoptotic rate in Hep G2 cells to a peak of 32.2%. It inhibited the growth of Hep G2 cells by arresting the cell cycle in the S stage, resulting in the lack of the cell population in the G2/M phase, and suppressing the anti-apoptotic protein Bcl-2 [19]. Additionally, α -solanine exhibited cytotoxic properties on SW480, SW620, HT-29 and MCF-7 cell lines. It inhibited

their growth, movement, and invasion while promoting death by arresting the cell cycle [20, 21].

Niosome NPs offer various significant benefits for solanine delivery in comparison to other NP technologies. The restricted water solubility of solanine, a significant barrier to its therapeutic application, is substantially mitigated by the unusual bilayer structure of niosomes, which facilitates the incorporation of both hydrophilic and hydrophobic substances, hence improving solanine's solubility and bioavailability. Today's breast cancer therapies often exhibit systemic toxicity and limited drug distribution at the tumor, resulting in reduced efficacy and undesirable side effects. Solanine, despite its potential anti-cancer activity, encounters obstacles due to its insufficient solubility and rapid degradation, which hinders its therapeutic use. Niosomes mitigate these significant shortcomings by: (1) inhibiting solanine degradation in physiological environments, thereby facilitating transport to tumor tissue; (2) enabling precise distribution of the drug, which enhances efficacy while reducing off-target toxicity; and (3) providing regulated solanine release, thereby prolonging therapeutic effect and potentially reducing dosing frequency. The synergistic advantages of enhanced solubility, protective mechanisms, targeted delivery, controlled release, biocompatibility and versatility make solanine-loaded niosomes a viable approach to address the shortcomings of existing breast cancer therapies and offer a potential avenue for more effective and less toxic treatment alternatives. The aim of this work was to develop solanine-loaded niosome NPs (SN-NPs) based on the recognized anti-cancer and anti-metastatic properties of solanine. Following synthesis, the anticancer and anti-metastatic properties of these SN-NPs were evaluated against a BC cell line.

Materials and methods

Fabrication of niosomes/solanine NPs

Niosome NPs were synthesized using the thin-layer hydration approach [22]. Briefly, a solution of chloroform and methanol was prepared in a ratio of 2:1 to a volume of 50 mL (solution 1). Then span60 (0.5 mL), Tween 60 (0.5 mL) and cholesterol (0.5 g) were added in a ratio of 1:1:1 to a volume of 50 mL (solution 2). In the next step, solution 1 (20mL) and solution 2 (20mL) were mixed together in a ratio of 1:1 to a total volume of 40 mL. Then it was placed at a temperature of 90 °C and 150 rpm until the complete evaporation of the solvent (20–30 min) and the creation of a thin lipid layer. After this cycle, a lipid layer forms as a thin coating on the surface of the balloon. In the next step, 90 mL of PBS with pH 7.4 was prepared and added to the container containing the lipid layer (hydration step) and homogenized by a magnetic stirrer for 30 min at 70 °C (solution 3). Then 40 mg of solanine was added to distilled water and stirred for

10 min (solution 4). Solution 4 was then added dropwise to solution 3 for 24 h at 150 rpm and 60 °C using an infusion set. Solanine-loaded Niosome NPs were synthesized. After hydration, the plates were sonicated for 15 min at 80% power to reduce particle size.

Characterization of SN-NPs

The SEM (ZEISS LEO-1430 VP, Germany) was applied to analyze the morphological features of the produced niosome-loaded solanine NPs. Additionally, dynamic light scattering (DLS, K-ONE Inc., Korea) was employed to ascertain the size of NPs. The suspension was diluted with deionized water to achieve the desired volume, and subsequently, the analysis was conducted at a temperature of 25 °C. The average particle size of the NPs, PDI and zeta potential were measured using a zeta sizer instrument at a wavelength of 633 nm and a temperature of 25 °C. The measurements were based on DLS. To investigate the relationship between different components of niosome NPs and solanine, we used FTIR using Spectrum Two, Perkin Elmer, USA and the KBr disk method. Scanning was performed on the samples between 4000 and 400 cm^{-1} [23].

Encapsulation efficiency (EE)

The effectiveness of encapsulation was evaluated using spectroscopic techniques. The concentration of solanine encapsulated in the niosome NPs was determined using a UV spectrophotometer (Shimadzu, Japan). In this assay, the amount of drug initially added was 40 mg/10 mL, and the OD averaged 2.29 from 3 replicates. Similarly, the OD of the free “untrapped drug” averaged approximately 0.405 from 3 replicates (Supplementary Material 1). The entrapment efficiency was determined using the following equation [24]:

$$\text{Encapsulation Efficiency (\%)} = \left[\frac{(\text{Drug added} - \text{Free nentrapped drug})}{\text{Drug added}} \right] \times 100$$

In vitro release study

Two sealed dialysis bags (10 K MWCO, Gibco, USA) containing 1 mL of SN-NPs, free niosomes, and free solanine were immersed in two beakers containing 100 mL of PBS buffer with pH values of 5.2 and 7.4. The buffer was agitated at a constant speed of 150 rpm at a temperature of 37 °C. At certain intervals, 1 mL of the solution was eliminated and substituted with a new buffer. The discharge percentage indicates the proportion of the medication released in the buffer medium. The rate of medication released was determined by measuring the ratio of the quantity of formulations released in a dialysis bag to the total amount of drug, utilizing UV measurements at 760 nm [25].

Cell culture

The MCF-7 cell line (HTB-22), obtained from the Pasteur Institute of Iran, is characterized by being estrogen receptor (ER) positive, progesterone receptor positive, and HER2 negative. The human breast epithelial cell line MCF10A, the most common natural breast cell model, was obtained from Pasteur Institute of Iran, with access code CRL-10,317. The cells were grown in DMEM/F12 high glucose medium (DACell, Iran) supplemented with 10% fetal bovine serum (FBS, Gibco), 100 IU/mL penicillin, and 100 $\mu\text{g}/\text{mL}$ streptomycin (Sigma-Aldrich). The culture was maintained in a 5% CO_2 atmosphere at 37 °C. The cells were collected by treating them with a solution of 0.25% trypsin-EDTA (DACell, Iran). After centrifugation, the cells were counted and then submerged in PBS for the subsequent experiment.

MTT assay

MCF-7 and MCF-10 cells were cultivated and then placed in 96-well plates at a density of 10^4 cells per well. The plates were filled with a mixture of DMEM/F12, which included 1% penicillin-streptomycin and 10% FBS. The cells were then incubated in an environment with 5% CO_2 . Various quantities of niosomee, solanine, and solanine-loaded niosomees (ranging from 40 to 0.3122 mg/100mL) were applied to 96-well plates in 3 duplicates. The highest concentration of the synthesized compound was used in this study for the upper threshold (40 mg). It was then diluted in a fixed ratio up to 8-fold by serial dilution. A fixed dilution factor (a two-fold logarithmic progression) ensures a balanced distribution of data points across different concentrations. It increases the likelihood of obtaining the full range of biological activity from minimal to maximal effects.

The plates were then incubated for 24, 48 and 72 h at 37 °C in an incubator with 5% CO_2 . The time intervals chosen were to allow for both immediate and delayed cytotoxic effects. The 24-hour interval facilitated the assessment of immediate cellular responses, while the 48- and 72-hour intervals showed the prolonged effects of SN-NPs on cell survival and proliferation. The prolonged observation time was essential to understand the lasting consequences of solanine release from niosomes and the cumulative impact on cell viability. Following the incubation period, 100 μL of MTT solution (0.5 mg/mL in PBS) was introduced into the wells and left to incubate for 4 h at 37 °C in a 5% CO_2 incubator. The liquid portion was extracted and 100 μL of DMSO was introduced to dissolve the formazan crystals produced by the viable cells. Ultimately, the ELISA Reader (ChroMate, Netherlands) was used to determine the absorbance of the specimens at a wavelength of 570 nm. The rate of cytotoxicity was determined by comparing the absorbance of the treated cells with that of the control cells. MCF-10 is considered

a normal cell line. Tamoxifen drug was considered a positive control. Tamoxifen is a recognized and extensively used positive control in BC research, especially with MCF-7 cells. This enables us to compare the efficacy of our new SN-NPs with a recognized and therapeutically relevant anti-cancer drug [26].

$$\text{Viability (\%)} = \frac{(\text{A treatment} - \text{A blank})}{(\text{A control} - \text{A blank})} \times 100$$

Investigation of apoptosis

The Annexin V-FITC/PI double staining method was used to evaluate cell apoptosis after sample application. Before treatment, MCF-7 cells (5×10^5 cells/well) were incubated overnight in 6-well plates and exposed to IC_{50} doses of niosome/solanine NPs, free solanine, and free niosome for 72 h. Following two washes with cold, sterile PBS (pH 7.4), 5×10^5 cells were suspended per well in a 6-well plate using the 1X binding buffer supplied by the reagent. The cells were treated as directed by the manufacturer by adding specific quantities of annexin V-FITC (green fluorescence) and propidium iodide (red fluorescence) (Affymetrix, eBioscience, USA). The incubation period was 10 min at ambient temperature. The cell samples were transferred to a flow cytometric tube and analyzed via flow cytometry in the last phase.

Investigation of cell cycle arrest

The proliferation of cells was assessed by PI staining. The level of DNA is utilized to identify the stage of the cell cycle, with the binding of PI to DNA being directly proportionate to the amount of DNA present. The cells were placed in complete media in 6-well plates with a density of 1×10^6 cells per well. Following an overnight incubation and three rounds of washing with PBS, cells were exposed to free solanine, free niosomes, and SN-NPs for 72 h in a complete medium. Subsequently, the cells were gathered and preserved in 70% cold ethanol for one night at a temperature of 4 °C. Following this, the cells were treated with 450 μ L of PI solution (including

RNase) in the absence of light for a period of 20 min at room temperature. Finally, the cells were examined using flow cytometry. The experiments were replicated thrice. Tamoxifen drug was considered a positive control [27].

Evaluation of gene expression by qRT-PCR

The suppressive impact of medications may be attributed to the modulation of gene expression. The levels of *MMP2*, *CDH-1*, *Bax*, *Bcl2*, and *GAPDH* genes were quantified using real-time polymerase chain reaction (Ausdiagnostic, Australia) in the presence of various concentrations (IC_{50} concentration) of free solanine, free niosome, NS-NPs and Tamoxifen as positive control. The TriPure isolation reagent (Roche Applied Science, Germany) was used to collect total RNA from MCF-7 cells according to the manufacturer's directions. Nanodrops (IMPLEN, Germany) and agarose gel were used to ensure the quantity and quality of extracted RNA. The cDNAs were generated from 2 μ g of the entire RNA using reverse transcriptase with oligodT primers (Parstous, Iran) in a final reaction volume of 20 μ L, following the manufacturer's instructions. The temperature schedule was configured as follows: 25 °C (5 min for primer annealing); 42 °C (60 min); 85 °C (5 min); 4 °C (5 min). The primers were constructed based on National Center for Biotechnology Information database information. The primer sequences for the genes indicated above are provided in Table 1 for the forward and reverse directions. The qRT-PCR was performed using the sense and antisense primers on real-time PCR system. The $2^{-\Delta\Delta CT}$ technique was used to calculate fold changes in the control group. The tests were performed three times [28]. Gene expression values were standardized to the glyceraldehyde-3-phosphate dehydrogenase (*GAPDH*) gene. *GAPDH* was chosen as an endogenous control because it is uniformly expressed across different experimental conditions and cell types, including MCF-7 cells. This normalization step was critical to compensate for discrepancies in RNA input and qRT-PCR efficiency, thus enabling accurate measurement of target gene expression.

Statistical analysis

The tests in this research were replicated three times, and the outcomes were examined using GraphPad Prism version 8.0.2 software, which utilized a one-way analysis of variance. A significance level of $p < 0.05$ was deemed significant.

Results

Characterization of SN-NPs

Table 2 shows the size of NPs containing solanine. The average particle size and PDI of NPs are 50–70 nm and 0.452, respectively, as shown in Table 2. A PDI value of 0.452 for solanine-loaded niosome NPs is often regarded

Table 1 Primer sequences designed for qPCR

| Genes | Sequence | Tm | CG% |
|--------------|-------------------------|---------|-------|
| <i>MMP2</i> | F-AGTGGATGATGCCTTTGCTC | 60 °C | 50.0% |
| | R- GAGTCCGTCTTACCGTCAA | | 55.0% |
| <i>CDH-1</i> | F-CAGCACGTACACAGCCCTAA | 59.9 °C | 55.0% |
| | R- ACCTGAGGCTTTGGATTCCT | 60.1 °C | |
| <i>Bax</i> | F- GACGGCTCTCTCTACTT | 59.8 °C | 60.0% |
| | R- CTCAGCCCATCTTCTCCAG | 59.9 °C | 55.0% |
| <i>Bcl-2</i> | F-GGATTGTGGCCTTCTTTGAG | 59.7 °C | 50.0% |
| | R- GCCGGTTCAGGTACTCAGTC | | 60.0% |
| <i>GAPDH</i> | F-CGAGATCCCTCAAATCAA | 60.0 °C | 45.0% |
| | R- TTCACACCCATGACGAACAT | 59.8 °C | 45.0% |

Table 2 Analysis of niosome NPs containing solanine. Determination of hydrodynamic diameter of niosome-solanine NPs by DLS and zeta potential of niosome-solanine NPs with zetasizer

| Row | Test | Analysis | Threshold | Results |
|-----|----------------------------|----------|--|------------|
| 1 | Polydispersity index (PDI) | 0.452 | 0.1 to 0.25 most acceptable 0.25 to 0.5 acceptable 0.5 to 0.75 poor acceptable 0.75 to 1.00 not acceptable | acceptable |
| 2 | Surface charge (mV) | 60.7 mV | *The general dividing line between stable and unstable suspensions is generally taken at either +30 or -30 mV. Particles with zeta potentials more positive than +30 mV or more negative than -30 mV are normally considered stable. | stable |
| 3 | FeSEM (nm) | 26 nm | **Typically, they have a size between 1 and 100 nm that permits a longer circulation half-life in vivo. | Good |
| 4 | DLS (nm) | 50–70 nm | | Good |

*<https://www.research.colostate.edu/wp-content/uploads/2018/11/ZetaPotential-Introduction-in-30min-Malvern.pdf>

**Adamo G, Campora S, Ghersi G. Functionalization of NPs in specific targeting and mechanism release. In Nanostructures for novel therapy 2017 Jan 1 (pp. 57–80). Elsevier

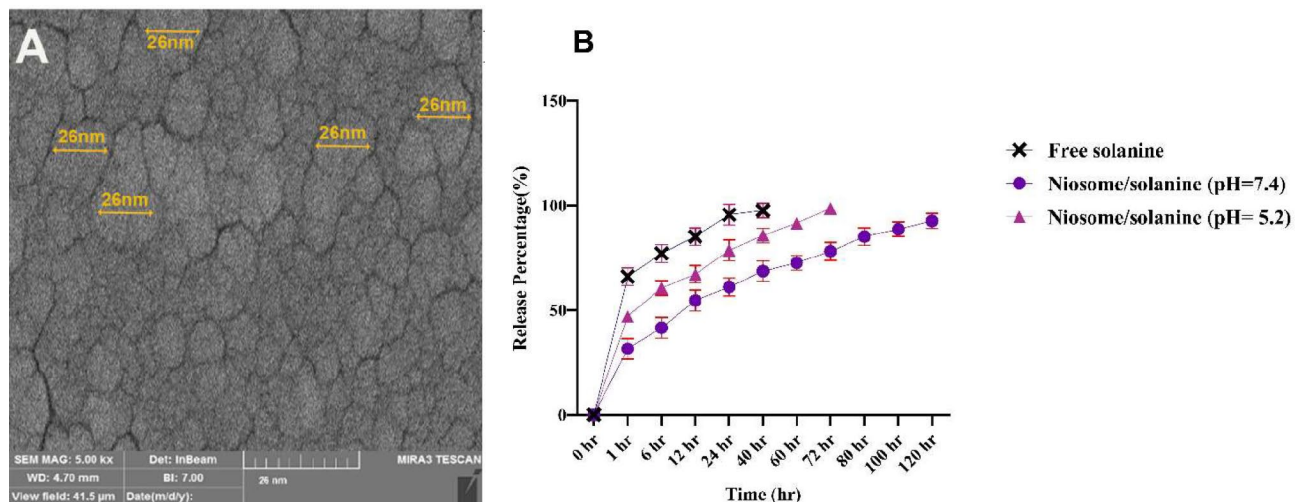


Fig. 1 Analysis of niosome NPs containing solanine. **(A)** Morphological analysis of solanine-niosome NPs using SEM. SEM imaging results indicate that SN-NPs possess advantageous characteristics for the cellular transport of solanine. The diminutive size, spherical morphology, and smooth surface all suggest a meticulously engineered nanoparticle delivery mechanism. **(B)** Release pattern of free solanine and niosome NPs containing solanine at pH 5.2 and 7.4 after 120 h. The research revealed a considerably quicker release of solanine from the niosomes at pH 5.2 compared to pH 7.4. This shows that the niosomes are more likely to discharge their cargo in a more acidic environment

as acceptable, however indicative of a more wider size dispersion. Lower PDI values signify a more homogeneous size distribution, whilst elevated values imply a broader spectrum of particle sizes. A PDI under 0.5 indicates that the majority of solanine-containing niosome NPs fall within an acceptable size range. SEM was used to evaluate the morphological characteristics of the most favorable SN-NPs. Figure 1A shows a SEM image of the improved formulation. This image shows a stable spherical shape and smooth surface, with an average size of less than 26 nm and no visible bulk component. As previously mentioned, we quantified the zeta potential of SN-NPs using a Zeta Sizer. Table 2 displays the zeta potential of niosome NPs containing solanine, which is measured to be 60.7 mV. The results corroborated the existing nanosystem's accurate size distribution and zeta potentials. Positively charged NPs may adhere to the negatively charged surfaces of cancer cells via electrostatic

interactions, possibly facilitating increased cellular absorption and tailored medication administration. The long-term stability of SN-NPs was assessed by monitoring particle size, polydispersity index (PDI) and zeta potential during 120 h. The results showed little change in particle size and PDI, indicating robust physical stability. The zeta potential was consistently high [+60 mV], indicating that the electrostatic stability of the SN-NPs was maintained throughout the time. The prolonged stability is essential for ensuring the efficacy and durability of SN-NPs in future clinical applications.

Investigation of FT-IR results

An FTIR examination was conducted to verify the presence of solanine in the nano-niosome formulation. Table 3 displays the FTIR spectra of the unbound niosome and SN-NPs. The FTIR spectrum of the blank niosome (Table 3) exhibits distinct peaks corresponding to

Table 3 Fourier-transform infrared (FTIR) spectra of blank niosome and niosome containing solanine

| Nanoparticle | Wavelength | Connection bonds | Results |
|-----------------------------|---------------------------------|---------------------|--------------------|
| Blank niosomee | 3553.84 cm^{-1} | O–H bonds | cholesterol |
| | | N–H bonds | Tween-60 |
| | 1892.42 cm^{-1} | C–O bonds | Tween-60 or span60 |
| | 3013.13 cm^{-1} | -OH bonds | span 60 |
| | 2929.70 cm^{-1} | C–H bonds | span 60 |
| | 1638.01 cm^{-1} | -COO bonds | span 60 |
| Niosome containing solanine | 3548.73 cm^{-1} | -OH bonds | cholesterol |
| | 2923.76 cm^{-1} | C–H bonds | span60 |
| | 1637.72 cm^{-1} | -COO bonds | Tween-60 or span60 |
| | 1600 cm^{-1} | -OH bonds | solanine |
| | 1093.91–618.86 cm^{-1} | C–H, C–O, C–N bonds | solanine |

span 60, Tween-60, and cholesterol in the wavelength region of 3553–475 cm^{-1} . The band seen at 3553.84 cm^{-1} was attributed to the presence of cholesterol and Tween-60, explicitly indicating the stretching of O–H bonds in phenols and N–H bonds in secondary amines. The presence of the carbonyl group in Tween-60 and span60 is characterized by a prominent absorption band at 1892.42 cm^{-1} , which arises from the stretching vibration of the C–O bond. The peaks of 3013.13, 2929.70 and 1638.01 cm^{-1} , related to the presence of -OH, C-H and -COO groups, respectively, indicate span 60 in niosome compound. The solanine-niosome NPs exhibited peaks at waves 3548.73, 2923.76, and 1637.72 cm^{-1} , indicating the presence of -OH, C-H, and -COO groups, respectively (Fig. 2B). The SN-NPs exhibit a more distinct and intense band in the 1600 cm^{-1} area and larger bands in 1093.91–618.86 cm^{-1} regions, as compared to the blank niosome. The SN-NP spectrum exhibited a more pronounced and intense band in the 1600 cm^{-1} region compared to the blank niosome. This region is often associated with C=C stretching vibrations, which could be present in the solanine structure. The SN-NP spectrum showed more prominent bands in the 1093.91–618.86 cm^{-1} region. This region is complex and can contain contributions from various functional groups, including C–O stretching, C–N stretching, and C–H bending. Solanine, being a complex molecule, likely possesses such functional groups. The increased prominence of these bands in the SN-NPs spectrum, compared to the blank niosome, suggests the presence of additional functional groups contributed by solanine.

Entrapment efficiency and release profiles

Encapsulation effectiveness is a crucial physicochemical metric in niosome formulations. Prior studies have shown that niosomes created using the thin film approach had a greater encapsulation efficiency than those produced using other methods. The drug's accessibility is guaranteed by the superior entrapment efficiency, resulting in an enhanced quantity of solanine inside the

particle at more excellent EE. The encapsulation efficiency for solanine was 82.3%±0.24% (Supplementary materials 1), demonstrating the effective incorporation of solanine into niosome NPs. The drug release investigation was performed at two pH levels, 7.4 and 5.2, to replicate physiological circumstances and the tumor microenvironment, respectively (Fig. 1B). A pH of 7.4 denotes the physiological pH of blood and healthy tissues, establishing a standard for medication release under typical settings. It is essential to evaluate premature medication leakage throughout circulation prior to reaching the target location. A pH of 5.2 replicates the acidic conditions typical of the tumor microenvironment, such as the extracellular space around MCF-7 tumor cells and the endolysosomal compartments inside the cells. A double-stage release of solanine was seen in both laden formulations, consisting of a relatively fast release of medication accompanied by a steady plateau or a delayed release phase. A release profile indicates that the niosome formulation exhibited a notably monitored release of solanine for several hours, whereas 63% of the free solanine was released after 1 h (pH=7.4). At a physiological pH, the solanine NPs exhibited an initial rapid release of 35% of solanine after 1 h. Subsequently, about 51% and 90% of solanine were released after 12 and 120 h, respectively. The key finding is that the niosomes control the release of solanine. While free solanine shows a rapid release (63% in 1 h at pH 7.4), the niosome-encapsulated solanine releases much more slowly (35% in 1 h at pH 7.4). This sustained release is beneficial for maintaining therapeutic drug levels over a longer period and reducing the frequency of administration. On the other hand, the medication was released more rapidly at pH 5.4. Around 45% of the solanine was released from the NPs after 1 h, and the complete release of the drug was achieved in only 72 h. The study observed a significantly faster release of solanine from the niosomes at pH 5.2 compared to pH 7.4. This indicates that the niosomes are more likely to release their payload in a more acidic environment. The faster release at pH 5.2 (complete release in

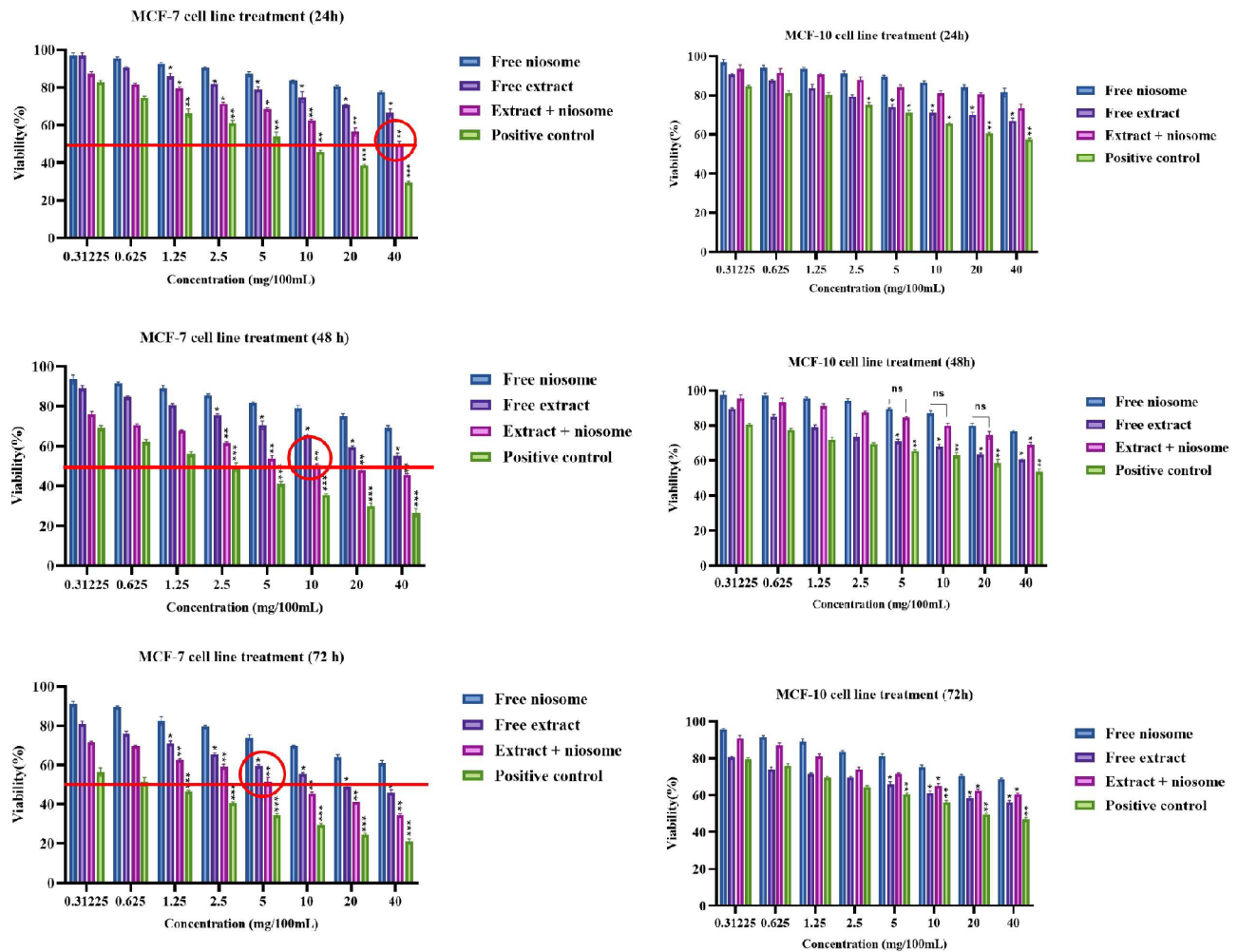


Fig. 2 The cytotoxic effect of free solanine, free niosome and solanine-loaded niosome NPs on MCF-7 and MCF-10 cell lines. The results of the MTT assay show that the toxicity of solanine-loaded niosome NPs is time- and dose-dependent and that with increasing time from 24 to 72 h, cell viability decreases in the group treated with solanine-loaded niosome NPs. The data are expressed as a percentage of cell viability, with the standard deviation (SD), ($n = 3$). * $p < 0.05$, ** $p < 0.01$, *** $p < 0.001$

72 h) compared to pH 7.4 (90% release in 120 h) suggests that the niosomes might be designed to release their payload in response to changes in pH. The released research aimed to illustrate the pH-responsive characteristics of the solanine-loaded niosomes, validating their capacity to release solanine in the acidic tumour microenvironment selectively. The noted discrepancies in pH 7.4 and 5.2 release profiles provide enough data to substantiate this assertion. The markedly accelerated release at pH 5.2, reflecting the tumour's acidic environment, substantiates the niosomes' capability for tailored drug delivery. Due to the evident and significant disparities in release kinetics at the two pH values, further kinetic modelling was considered superfluous for the objectives of this investigation.

Assessment of cytotoxicity

Figure 2 shows the survival rate of MCF-7 and MCF-10 cell lines after exposure to free solanine, free niosome, solanine loaded in niosome NPs and positive control (Tamoxifen) for 24, 48 and 72 h with different concentrations. Compared with control cells, the viability of MCF-7 cells was significantly decreased by niosome-loaded solanine in a time and concentration-dependent manner (** $p < 0.001$). IC_{50} values for MCF-7 cells exposed to solanine loaded in niosome NPs were 40 mg/100 mL. However, these values decreased to 10 mg/100 mL after 48 h and 5 mg/100 mL after 72 h. Tamoxifen, used as a positive control, exhibited IC_{50} values of 5 mg/100 mL at 24 h, 2.5 mg/100 mL at 48 h, and 0.625 mg/100 mL after 72 h of treatment. Compared to solanine loaded in Niosome NPs and tamoxifen, free Niosome NPs showed no significant effect on MCF-7 cell survival. The free solanine extract at a concentration of 40 and 20 mg/100 mL

showed minimal toxicity after 24 h. However, after 48 h, these concentrations significantly reduced the survival rate of MCF-7 cells. The data clearly show that solanine in niosomes exhibits significant cytotoxicity compared to free solanine at an earlier time point (24 h). The IC_{50} values for the niosome formulation decrease over time, indicating increasing efficacy. Free solanine, on the other hand, shows minimal toxicity after 24 h (Fig. 2). Niosome-encapsulated solanine was less toxic to the normal cell line MCF-10 than free solanine. Free niosome NPs showed no significant toxic effect on the normal cell line. However, the survival rate of MCF-10 cells treated with solanine-loaded NPs was 78% and 80% after 24 h at concentrations of 40 and 20 mg/100mL, respectively. In addition, the survival rate of MCF-10 cells treated with NPs containing solanine in these concentrations showed a significant decrease with increasing time. Furthermore, the toxicity findings of unbound niosomes on MCF-7 and MCF-10 normal cell lines indicate that it has no noteworthy negative impacts on the cell lines, thus demonstrating its biocompatibility.

Apoptosis assay

We used an apoptosis detection kit to determine the manner of cell death produced by solanine, free niosomes, and solanine-loaded niosome nanoparticles (SN-NPs) in MCF-7 cells. Cells were subjected to each treatment at their corresponding IC_{50} concentrations for 72 h, after which apoptotic levels were assessed using flow cytometry. The data obtained was examined via a four-Q gating strategy: Q_1 denoting necrotic cells, Q_2 indicating late apoptotic cells, Q_3 signifying early apoptotic cells, and Q_4 representing viable cells. This test utilizes Annexin V's strong affinity for phosphatidylserine, an early marker of apoptosis, which was identified using FITC. Propidium iodide (PI), a DNA-binding dye, was used to differentiate necrotic cells from apoptotic cells, since it can penetrate only those cells with damaged membranes. Figure 3 demonstrates the prompt occurrence of apoptotic effect ($Q_2 + Q_3$) in MCF-7 cells upon exposure to niosome NPs containing solanine. The most striking difference is the significantly lower percentage of live cells in the SN-NPs group (46.80%) compared to the free solanine group (83.70%). This suggests that the solanine-loaded NPs have a much stronger effect on reducing cell viability. This study found that niosome and blank solanine extract, at a concentration known as IC_{50} , did not significantly affect the survival rate of MCF-7 cells compared to the control group. A survival rate of 98.6% was observed in MCF-7 cells treated with niosome at the IC_{50} concentration. The highest primary and secondary apoptosis rates of 15.33% and 33.10%, respectively, were observed in MCF-7 cells treated with niosome NPs containing solanine, which showed a significant difference

with free solanine and free niosome ($p < 0.01$). Following a 72-hour treatment with niosomes containing solanine, over 30% of MCF-7 cells were shown to be in the late apoptotic stage, while 5.06% were found to be at the necrosis phase. The SN-NPs demonstrate superior efficacy as a delivery method for solanine, facilitating both early and late-stage apoptosis, hence diminishing cell viability ($p < 0.01$). In our flow cytometry analysis, primary apoptosis (Annexin V+/PI-) indicates early apoptosis, while secondary apoptosis (Annexin V+/PI+) signifies late apoptosis and maybe early necrosis. SN-NPs enhanced both, suggesting their pro-apoptotic influence on MCF-7 cells. The lowest survival rate (16.40%) and the highest secondary apoptosis rate (64.40%) of MCF-7 cells were observed in the group treated with tamoxifen (positive control), which showed a significant difference compared to other groups ($p < 0.01$). These data indicate that SN-NPs promote apoptosis in MCF-7 cells by different pathways. Annexin V staining indicates activation of the extrinsic apoptosis pathway, which involves death receptor signalling. The late apoptosis and necrosis observed could be due to the intrinsic apoptosis pathway facilitated by mitochondrial dysfunction. Further studies are needed to clarify the exact molecular pathways, including analysis of Bcl-2 family proteins. Evaluation of the expression of Bcl-2 family proteins (Bax, Bcl-2) to determine changes in mitochondrial membrane potential and the role of the intrinsic pathway. We used the real-time PCR method for the (Bax, Bcl-2) measurement.

Investigation of cell cycle modifications

Flow cytometry was used to assess cell cycle alterations in MCF-7 cells after treatment with IC_{50} doses of free niosome, free solanine, niosome NPs loaded with solanine, and tamoxifen (Fig. 4). Both SN-NPs and tamoxifen, a well-known anti-cancer medication, caused cell cycle arrest in the G0/G1 phase while decreasing the fraction of cells in the G2/M phase. This shows that SN-NPs may have similar anti-cancer properties as tamoxifen. In the treatment group with NPs loaded with solanine, 81% of the cells stopped in the G0/G1 phase and only 12% of the cells managed to enter the G2/M phase ($p < 0.01$). Persistent arrest in G0/G1 may induce apoptosis, or programmed cell death, in MCF-7 cells. This consequence is advantageous in cancer treatment, since it results in the eradication of malignant cells. The results showed that the encapsulation of solanine in niosomes significantly increases its ability to induce apoptosis and stop the cell cycle in the G0/G1 phase of MCF-7 cells compared to free solanine.

Evaluation of gene expression

Analysis of MCF-7 cells treated with solanine-niosome NPs and the positive control using quantitative real-time

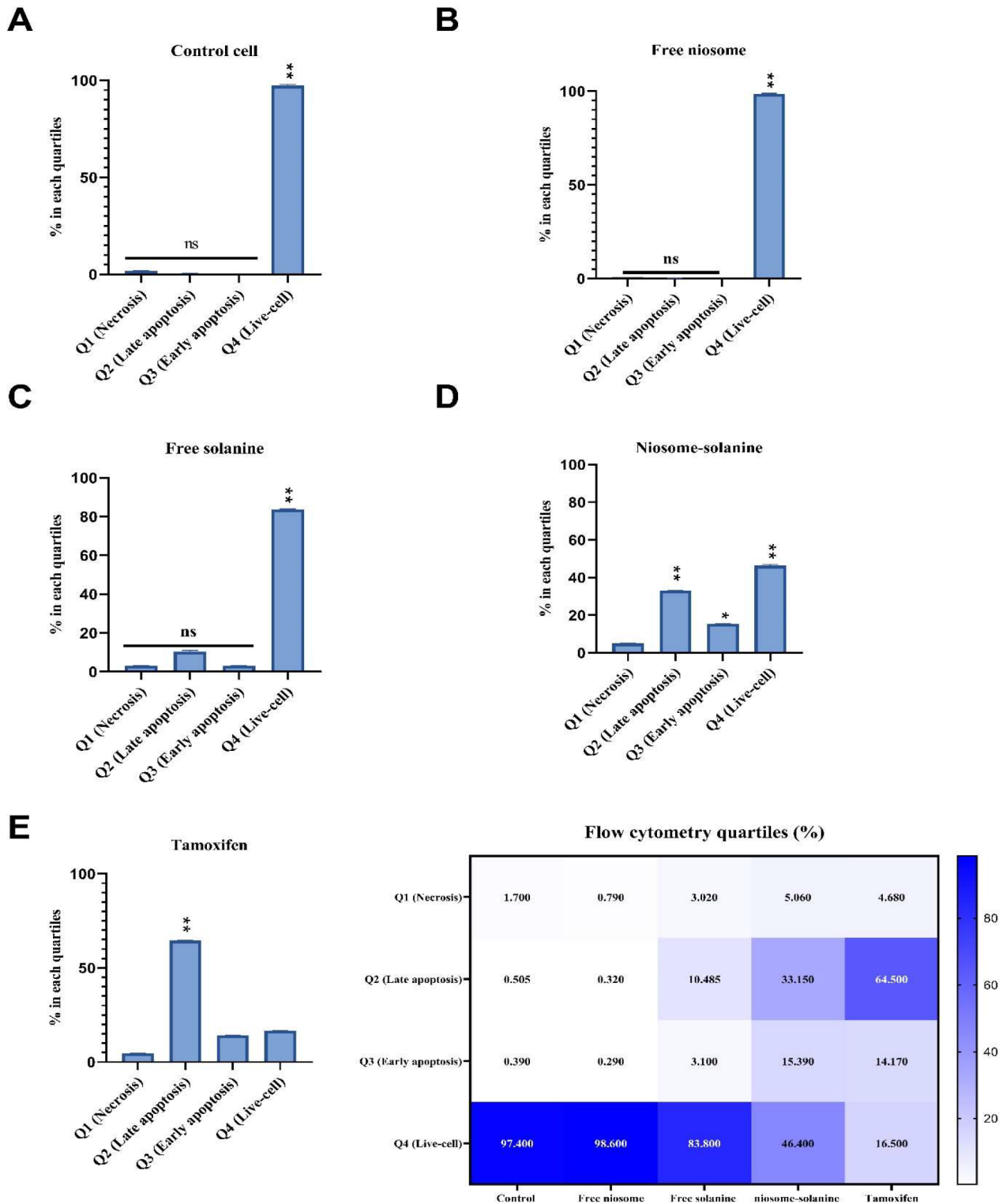


Fig. 3 Flow cytometric analysis of MCF-7 cells after exposure to IC_{50} concentration of different substances. (A) Control treatment, (B) Free niosome, (C) Free solanine extract, (D) niosome containing solanine extract and (E) Tamoxifen. Q₁ represents necrotic cells, Q₂ represents late apoptotic cells, Q₃ represents early apoptotic cells, and Q₄ represents viable cells. The main discovery is that SN-NPs substantially enhanced apoptosis in MCF-7 cells relative to free solanine or free niosomes. Free solanine and free niosomes at their IC_{50} concentrations had no significant effect on the survival rate of MCF-7 cells in comparison to the control

Cell cycle

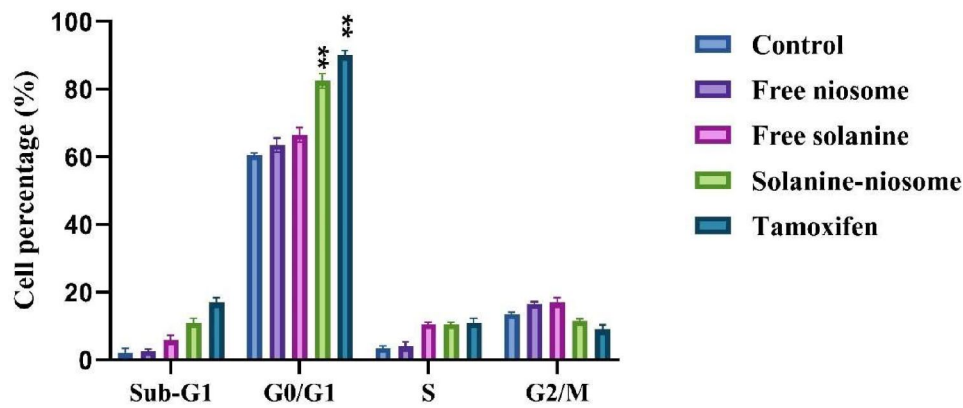


Fig. 4 The results of the analysis of cell cycle changes in MCF-7 cells after treatment with free niosome, free solanine, niosome NPs containing solanine and tamoxifen using flow cytometry. Results are displayed as mean ± SD, n = 3. * indicates a significant difference from the untreated control group. p < 0.01**

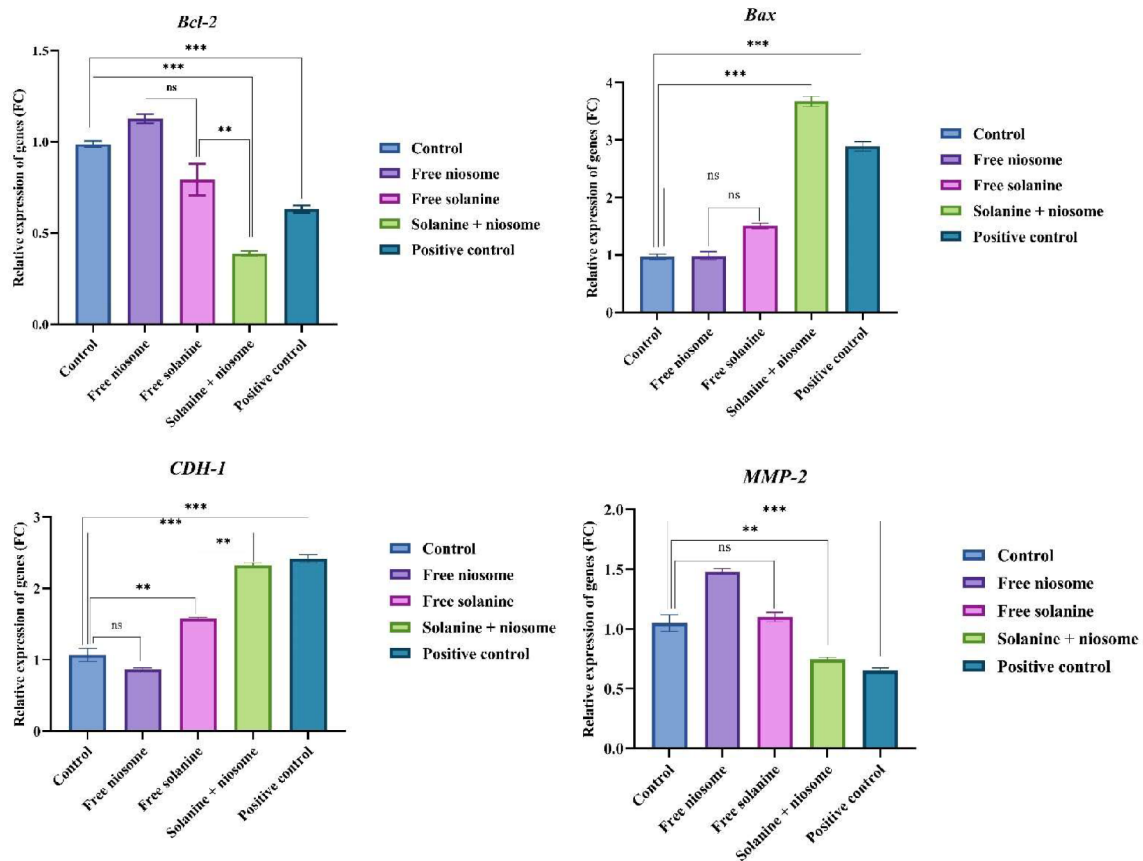


Fig. 5 Evaluation of *Bax*, *Bcl-2*, *CDH-1* and *MMP2* gene expression changes in MCF-7 cells treated with free solanine, free niosome, solanine-niosome NPs and tamoxifen as a positive control using real-time PCR. The study results are mean ± SD and repeated three times. *** p < 0.001, **** p < 0.0001, ns: not significant

RT-PCR revealed increased levels of *Bax* and *CDH-1*. This indicates that these specific genes are important in apoptosis and metastasis. The transcription levels of *Bax*, *Bcl-2*, *CDH-1*, and *MMP2* genes were analyzed

using qPCR, with GAPDH as a reference control gene (housekeeping gene) (Fig. 5). All potential genes among different treatment groups observed a significant variation in expression. After treatment with NPs containing

solanine, the level of *Bax* and *CDH-1* gene expression in malignant cells was significantly higher compared to free niosomes and free solanine (**** $p < 0.0001$). It is accepted that *Bax* acts as a protein that suppresses tumor growth. Our investigation found that the *CDH-1* gene was considerably increased in expression in solanine-niosome and positive control treatment groups, compared to the free niosome, free solanine and control group (*** $p < 0.001$). Conversely, the increase in *CDH-1* expression was noticeable in cell lines treated with tamoxifen. Our findings showed that *Bcl-2* exhibited significant changes in MCF-7 cells treated with solanine-loaded NPs, as demonstrated by qRT-PCR analysis. The expression of *Bcl-2* in this group showed a significant decrease compared to niosome and free solanine (*** $p < 0.001$). The results of our study indicate that the expression of the *MMP2* gene in cancer cells treated with solanine-containing NPs is markedly decreased compared to those treated with solanine alone or niosome. This suggests the medicine has been successfully administered to the specific cancer cells (** $p < 0.01$).

We performed pathway analysis to gain more insight into the biological processes affected by SN-NPs. This investigation revealed that the changes in the expression of *Bax*, *Bcl-2*, *CDH-1* & *MMP2* are associated with many critical signaling pathways, including: The increase in *Bax* and down-regulation of *Bcl-2* indicate activation of the intrinsic apoptotic pathway, likely due to disruption of mitochondrial membrane potential. The overexpression of *CDH-1* indicates a possible reversal of epithelial-mesenchymal transition (EMT), a critical process in the spread of cancer. The down-regulation of *MMP2* indicates the suppression of ECM degradation, a critical factor for tumor invasion and metastasis. The PI3K/Akt/mTOR signaling pathway is prevalent in several malignancies, and alterations in apoptosis-related genes and *MMP2* may indicate alterations in this pathway. The MAPK pathway is prevalent in several malignancies, and alterations in apoptosis-related genes and *MMP2* may indicate alterations in this pathway.

Discussion

Cancer continues to represent a significant global health burden, with mortality rates persisting despite therapeutic breakthroughs. This underscores the need for new therapeutic approaches [26]. Natural chemicals, including solanine, have emerged as potential anticancer drugs and have shown antitumor activity in various cancers [27]. Solanine, a glycoalkaloid, has shown potential anticancer properties by inhibiting the development and proliferation of malignant cells [29]. Research has shown that solanine induces apoptosis in hepatocarcinoma cells, highlighting its potential as an economical cancer therapy. However, its insufficient water solubility limits its

bioavailability and therapeutic efficacy. We investigated niosomes as nanocarriers for the delivery of solanine to MCF-7 breast cancer cells [28]. This work involved the synthesis of new solanine-loaded niosome nanoparticles (SN-NPs) using Span 60, Tween 60 and cholesterol, followed by an evaluation of their cytotoxic effect on MCF-7 and MCF-10 cells by MTT assays. Characterization tests confirmed the effective production of nanoparticles and showed size distributions suitable for extensive circulation in the bloodstream [30]. The type of surfactant and the lipid mixture significantly influence the effectiveness of encapsulation and particle size [31]. SEM examination confirmed the spherical shape of SN-NP. The deviations between the particle size measurements with DLS and SEM are probably due to the different measurement principles. Scanning electron microscopy (SEM), an imaging technique for dry samples, provides direct measurements of the nanoparticle radius. DLS, an indirect technique, quantifies the hydrodynamic radius via particle motion, which can be influenced by dynamic accumulation and aggregation [32]. Our investigation revealed that the NP sizes measured in the SEM were below 30 nm, while the sizes measured in the DLS varied between 50 and 70 nm.

We investigated the physicochemical properties of solanine NPs, drug entrapment efficiency and drug release pattern. The encapsulation efficiency of solanine was $82.3\% \pm 0.24\%$. The release pattern of solanine from the niosome NPs was investigated by dialysis at pH 7.4 and 5.2. The results showed that the release of solanine from the NPs follows a two-stage pattern. The first stage shows a rapid increase in release within one hour at pH 7.4, followed by a slow and sustained release over 120 h, resulting in a solanine release of about 90%. The release of solanine at a pH value of 5.2, which is similar to the acidic environment of the lysosomes, is significantly faster than at a pH value of 7.4, with the entire solanine content being released within 72 h. The prolonged drug release of solanine niosome NPs means that these NPs can be used as an effective carrier for solanine delivery. Solanine release from niosome NPs is a pH-sensitive technique that aims to improve drug delivery to target areas such as the tumor microenvironment and lysosomes, which have lower pH values. At physiological pH (7.4), niosomes release solanine slowly and steadily, reducing premature drug loss in circulation. However, when exposed to the acidic environment (pH 5.2) found in the tumor microenvironment and lysosomes, the niosome structure alters, allowing for fast solanine release. This instability may include protonation of niosome components, resulting in changes to the bilayer structure and enhanced permeability. At pH 5.2, solanine is released more quickly and completely, ensuring that the therapeutic substance is efficiently supplied to cancer cells and maximizes its deadly impact. This tailored release

mechanism reduces off-target effects while increasing the therapeutic effectiveness of solanine. The cellular communication and absorption of NPs are significantly influenced by their surface charge [29]. SN-NPs showed a zeta potential of +60.07 mV, indicating the stability of the colloidal suspension of niosomes. Niosome NPs with zeta potentials above +30 mV or below -30 mV exhibit sufficient stability [30]. The polydispersity index quantifies the degree of homogeneity of particle size and measures the width of size dispersion. The PDI ranges from 0 to 1, with a lower value indicating a more homogeneous mixture. The homogeneous particles have a limited size range and show a low tendency to aggregate [31]. Our results show that probe sonication reduces the particle size of niosomes and thereby improves the efficiency of drug entrapment.

Liposomes, a widely used drug delivery method, are similar to niosomes in terms of bilayer architecture and drug encapsulation. However, niosomes have several advantages, including stability, cost-effectiveness, versatility, pH sensitivity and improved drug entrapment. Niosomes made from non-ionic surfactants have higher chemical stability than liposomes made from phospholipids, which are susceptible to hydrolysis and oxidation. This improved stability results in a longer shelf life and less drug leakage during storage and distribution. Niosomes are often less expensive than liposomes, making them a more economical choice for large-scale drug delivery. Niosomes offer more flexibility in surfactant selection and formulation, which facilitates optimization of drug release kinetics and targeted delivery. Niosomes can be synthesized from a wider range of materials. Although liposomes can be designed for pH-dependent release, as shown in our work, niosomes have inherently pH-dependent release characteristics due to the properties of nonionic surfactants. Sonication of the probe enabled high efficiency of drug entrapment in the niosomes [29–32].

In a study conducted with doxorubicin-loaded liposomes, it was found that the drug-loaded liposomes had a hydrodynamic size between 120 and 170 nm with a narrow distribution ($PDI < 0.2$) and covered a range of surface charges (-10.2 mV to +17.6 mV) [31]. These results were in agreement with the results of our study. However, our study showed that niosomes can generate smaller particles in terms of particle size. Moreover, the release of Dox from liposomes was lowest at pH 7.4 compared to acidic pH values [31]. Like the previous study, our study also showed that the release of the drug encapsulated in niosomes was better at acidic pH values. The MTT test was performed to determine the cytotoxicity of free niosomes, free solanine, and SN-NPs in MCF-7 cells. Free niosomes had no significant effect on MCF-7 cell viability compared to the control, showing that they

are biocompatible. After 24 h of incubation, free solanine at concentrations of 40 and 20 mg/100mL was found to be somewhat safe. However, after 48 h, these doses drastically decreased MCF-7 cell viability. Notably, SN-NPs showed considerable cytotoxicity at an earlier time point (24 h) than free solanine, suggesting improved transport and a faster commencement of action (Fig. 2).

The results of the study showed that in MCF-7 cells treated with *Solanum pseudo-capsicum* extract, the expression levels of *Bcl-2* and *Bax* genes decreased by 0.8-fold ($p < 0.05$) and 1.7-fold ($p < 0.01$), respectively. The overall apoptosis rate in this study was also 35.35% [21]. The results of the present study were consistent with the results of the previous study. However, the SN-NPs were able to alter the expression levels of the apoptotic gene *Bax* and the anti-apoptotic gene *Bcl-2* much more effectively.

When investigating the effects of α -solanine on cell viability, most studies have focused on different cell culture lines and confirmed our results [40, 41]. The IC_{50} concentrations of α -solanine in HepG2, SGC-7901 and LS-174 cells were 14.47, >50 and >50 $\mu\text{g/mL}$, respectively. HepG2 cells showed higher sensitivity to α -solanine [32]. The present study's findings on the anti-cancer activity of SN-NPs align and diverge in several ways with previous work on solanine-loaded chitosan NPs in MCF-7 cells. The isolated compound, solanine, and the chitosan-loaded solanine exhibited significant inhibitory activity against both MCF-7 and HMTV cancer cell lines. The determined IC_{50} values were 8.52 $\mu\text{g/mL}$ for solanine, 0.82 $\mu\text{g/mL}$ for the chitosan-loaded solanine, against MCF-7 cells. This study reported that solanine chitosan NPs induced both early and late apoptosis in MCF-7 cells [33]. Our results demonstrated that SN-NPs also induced both early and late apoptosis in MCF-7 cells. The cytotoxicity of *Solanum nigrum* extract was investigated in a separate study after 72 h of treatment against the MCF-12 A cell line and the luminal BC subtype A cell line MCF-7. The study demonstrated that the aqueous extract of *S. nigrum* L exhibited no cytotoxicity for normal breast MCF12A cells at concentrations of 5 g/L or 10 g/L. Conversely, it induced toxicity of 8% ($p > 0.05$) at 5 g/L and 43% ($p < 0.05$) at 10 g/L in BC MCF7 cells [34]. Niosome NPs have several potential benefits for the delivery of solanine in comparison to other NPs technologies. Their non-ionic characteristics often result in less toxicity and enhanced biocompatibility relative to charged nanoparticles, possibly mitigating the detrimental effects of solanine on healthy cells. Niosomes provide superior drug encapsulation efficiency and diverse drug loading capabilities, accommodating both hydrophilic and hydrophobic substances such as solanine. Moreover, their adjustable dimensions and surface characteristics provide regulated drug release and possible targeting

alterations, in contrast to some other nanoparticle varieties. Although free solanine may demonstrate considerable cytotoxicity against cancer cells, it also endangers normal cells, resulting in sensory discomfort and other harmful consequences. Niosome encapsulation seeks to reduce off-target effects by protecting solanine during transport and facilitating its release exclusively at the tumor site, hence possibly enhancing its therapeutic index. The remarkable anti-cancer activity of SN-NPs against MCF-7 cells and their lower toxicity to normal cells suggest a promising therapeutic potential for breast cancer therapy. The pH-sensitive release of solanine from niosomes in the acidic tumor microenvironment improves targeted drug delivery, reduces systemic toxicity and optimizes efficacy at the tumor site. The improved stability, biocompatibility and controlled release of SN-NPs offer a significant advantage over free solanine and other nanoparticle formulations. This improved nano-carrier technology can promote solanine bioavailability, minimize off-target effects and improve therapeutic outcomes for breast cancer patients.

The flow cytometric data showed that the cytotoxicity of solanine-loaded niosomes on MCF-7 cells was achieved by inducing apoptosis. Significantly, SN-NPs treatment decreased cell viability to 46.80%, in contrast to free solanine, which maintained a vitality of 83.70%. Neither free niosomes (98.6% viability at IC_{50}) nor free solanine had a significant impact on cell survival relative to the control. SN-NPs elicited the greatest rates of early (15.33%) and late (33.10%) apoptosis, greatly above those of free solanine and free niosomes ($p < 0.01$). This work presents solid evidence for the significant anti-cancer efficacy of SN-NPs against MCF-7 BC cells. Our results indicate that SN-NPs therapy successfully initiates apoptosis, a programmed cell death mechanism essential for the eradication of malignant cells, while concurrently inducing a substantial G0/G1 cell cycle halt. The noted rise in early and late apoptotic populations, together with the significant buildup of cells in the G0/G1 phase, highlights the dual effect of SN-NPs on MCF-7 cell viability. The substantial decrease in viable cell counts after SN-NPs therapy further substantiates the effectiveness of this therapeutic method.

The ratio between the levels of Bcl-2 and Bax proteins controls how cells respond to cell death-inducing signals by influencing the formation of pores in the mitochondrial membrane called the mitochondrial MTP hole [35]. The Bax/Bcl-2 ratio indicates the equilibrium between pro-apoptotic Bax and anti-apoptotic Bcl-2 proteins, which regulate mitochondrial outer membrane permeabilization and cytochrome c release, a crucial phase in apoptosis. An elevated Bax/Bcl-2 ratio signifies a transition towards apoptosis, as Bax's pore-forming function surpasses Bcl-2's inhibitory influence on cytochrome c

release [36]. *CDH-1*, or E-cadherin, is a transmembrane protein whose function depends on calcium and plays a critical role in the formation of certain intercellular junctions necessary for epithelial cell attachment [37]. *CDH-1* is a gene that plays an important role in the development of sporadic BC. *CDH-1* mutations are common in BC, especially in lobular breast tumors [38]. MMPs are a class of endopeptidases that are dependent on zinc for their activity. They have a crucial function in tissue remodeling by degrading components of the extracellular matrix, thus creating a favorable environment for cell development. Nevertheless, several MMPs are overproduced in various cancers to promote tumor cell growth and proliferation [39]. Consistent with previous research, our study confirms that the use of solanine loaded in niosome NPs has anticancer properties and effectively inhibits cell migration in MCF-7 BC cells. Furthermore, administration of solanine-containing NPs at IC_{50} concentration resulted in more than 3.5- and 2.5-fold upregulation of *Bax* and *CDH-1* genes in MCF-7 cells ($p < 0.001$), respectively. The expression of genes involved in cell migration and anti-apoptosis, such as *Bcl-2* and *MMP2*, was reduced in MCF-7 by 0.5-fold and 0.7-fold, respectively ($p < 0.001$). Our gene expression results correspond with recognized BC pathways: The upregulation of *Bax* and *CDH-1*, together the downregulation of *Bcl-2* and *MMP2*, signifies a transition towards apoptosis and diminished cell migration, which are critical therapeutic targets in breast cancer. These alterations indicate that SN-NPs stimulate pro-apoptotic pathways while inhibiting those that facilitate cell survival and metastasis, aligning with the intended effects of anti-cancer medicines. Modulating these genes is an established approach for addressing BC development. Previously, α -solanine had shown the ability to prevent the spread, movement and migration of human melanoma cells (A2058) by suppressing JNK, PI3K and Akt phosphorylation and NF- κ B activation and reducing the activity and expression of *MMP2/9*. The results of this study showed that the activities of pro *MMP9* and pro *MMP2* decreased significantly ($p < 0.01$) after treatment with α -solanine at concentrations of 13.8 and 18.4 mM for 24 h [40]. In a separate study, α -solanine reduced the production of oncogenic microRNA-21 by decreasing the expression of *MMP2/9* with a 1-fold change ($p < 0.01$) via the ERK and PI3K/Akt signaling pathways, thereby suppressing the invasion of human prostate cancer cells (PC-3) and increasing the expression of the tumor suppressor microRNA-138 [41].

SN-NPs has considerable clinical promise for cancer treatment owing to their improved delivery and targeted release functionalities. The observed enhancements in cellular absorption and cytotoxicity relative to free solanine indicate that SN-NPs may result in enhanced therapeutic effectiveness in vivo, possibly facilitating

superior tumor management and less systemic toxicity. The pH-sensitive release mechanism of SN-NPs facilitates tailored drug administration to the acidic tumor microenvironment, reducing off-target effects and enhancing the medication's efficacy on cancer cells while preserving healthy tissues. Moreover, the capacity of SN-NPs to cause apoptosis and cell cycle arrest underscores their potential as a significant element in combination cancer therapy, possibly enhancing the efficacy of current chemotherapeutics or other targeted strategies. Despite the encouraging preclinical outcomes, several difficulties remain before SN-NPs may be converted into therapeutic applications. Increasing the synthesis of niosome nanoparticles for large-scale production while ensuring uniformity in size, shape, and drug encapsulation is a considerable challenge. Maintaining the long-term stability of nanoparticles during storage is essential, since aggregation, drug leaking, or alters in particle size might impact their effectiveness and safety. The absence of in vivo investigations is a significant constraint. Although our in vitro results are promising, it is crucial to investigate the activity of SN-NPs in animal models to evaluate their effectiveness, biodistribution, and possible toxicity in vivo. These investigations will be essential for establishing the best dose, delivery method, and long-term effects of SN-NPs, hence facilitating clinical trials and their prospective use in human cancer therapy.

Although our in vitro results suggest promising anti-cancer efficacy of SN-NPs, several limitations must be acknowledged, particularly regarding in vivo translation, complexity of in vitro and in vivo studies, pharmacokinetics and biodistribution, in vivo toxicity, tumor heterogeneity and drug resistance, scalability and manufacturing, and interactions with the immune system. Our study focused on MCF-7 cell lines, which may not fully mimic the complicated tumor microenvironment and heterogeneity in vivo. In vivo studies are critical to evaluate the efficacy and toxicity of SN-NPs in a more physiologically relevant context. The in vivo pharmacokinetics and biodistribution of SN-NPs are not yet known. Factors such as blood circulation, tissue penetration and in vivo drug release can influence therapeutic efficacy. Evaluation of nanoparticle accumulation in tumor tissue compared to healthy tissue is critical. Although the SN-NPs exhibited little toxicity in normal MCF-10 cells, in vivo toxicity studies are essential to determine potential systemic toxicity and off-target effects. The long-term consequences of NPs and solanine need to be investigated. Breast cancer exhibits considerable tumor heterogeneity, leading to possible resistance to therapy. In vivo research needs to investigate the efficacy of SN-NPs in different breast cancer subtypes and explore possible causes of drug resistance. The scalability and production of SN-NPs for clinical applications pose significant obstacles.

Improving the formulation and production process is critical to ensure consistent quality and efficacy. Research has not evaluated the interaction of nanoparticles with the immune system, which is an essential element of any in vivo application. Mitigating these limitations is essential for converting our in vitro discoveries into commercially applicable drugs. Future research should focus on in vivo efficacy and toxicity evaluations, pharmacokinetic and biodistribution studies, and optimization of SN-NP formulations for clinical use.

Conclusion

In this research, a novel niosomal delivery system for solanine, a phytochemical with potential anticancer activity, was developed and analyzed. The improved niosome formulation showed advantageous properties such as smaller size, higher entrapment efficiency and uniform, regulated drug release. In vitro studies with MCF-7 breast cancer cells showed that solanine-loaded niosomes significantly enhanced the anti-cancer effect of solanine compared to free solanine. Significantly, solanine-coated niosome nanoparticles induced apoptosis in MCF-7 cells equivalent to that of tamoxifen, a conventional breast cancer therapy. This enhanced activity was associated with the regulation of key genes involved in apoptosis and metastasis, resulting in increased cell mortality and reduced cancer spread. The results suggest that solanine-loaded niosomes may be a viable treatment approach for breast cancer. Future studies investigating solanine-loaded niosomes hold promise for the treatment of breast cancer, as they could potentially enhance drug delivery to tumor sites, improve cellular uptake of solanine, and reduce systemic toxicity compared to free solanine. This targeted approach could lead to more effective and less harmful therapeutic interventions. To realize this potential, further research is needed to optimize the niosome formulation and validate efficacy in preclinical and clinical settings.

Abbreviations

| | |
|--------|---|
| SN-NPs | Solanine niosome nanoparticles |
| NPs | Nanoparticles |
| PDI | Polydispersity index |
| BC | Breast cancer |
| HER2+ | Human epidermal growth factor receptor 2 positive |
| TNBC | Triple negative BC |
| BBB | Blood-brain barrier |
| Gas | Glycoalkaloids |
| SEM | Scanning Electron Microscope |
| FTIR | Fourier Transform Infrared Spectroscopy |
| PI | Propidium iodide |
| EE | Encapsulation efficiency |
| Q | Quadrant |
| MTP | Membrane permeability transition |
| MMPS | Matrix metalloproteinases |

Supplementary Information

The online version contains supplementary material available at <https://doi.org/10.1186/s12885-025-14249-y>.

Supplementary Material 1

Acknowledgements

None.

Author contributions

N.Z. conceptualized and wrote the manuscript. M.K. wrote the manuscript and did the necessary editing, supervised and performed the investigations and statistical analysis. E.A. wrote the manuscript. All authors read and approved the final manuscript.

Funding

None.

Data availability

The materials used in this study are available from the corresponding author upon request.

Declarations

Ethics approval and consent to participate

All the steps of this research have been done under the supervision of the National Committee of Ethics in Biomedical Research and it has the code of ethics number IRIAU.ET.REC.1402.023.

Consent for publication

Not applicable.

Competing interests

The authors declare no competing interests.

Received: 29 December 2024 / Accepted: 29 April 2025

Published online: 12 May 2025

References

- Tran P, et al. Recent advances of nanotechnology for the delivery of anticancer drugs for breast cancer treatment. *J Pharm Invest.* 2020;50:261–70.
- Passos JS, et al. Contributions of nanotechnology to the intraductal drug delivery for local treatment and prevention of breast cancer. *Int J Pharm.* 2023;635:122681.
- Bertucci F, et al. The therapeutic response of ER+/HER2– breast cancers differs according to the molecular basal or luminal subtype. *NPJ Breast Cancer.* 2020;6(1):p8.
- Giaquinto AN et al. Breast cancer statistics, 2022. *CA: a cancer journal for clinicians.* 2022; 72(6):524–41.
- Bailleux C, Eberst L, Bachelot T. Treatment strategies for breast cancer brain metastases. *Br J Cancer.* 2021;124(1):142–55.
- Lüönd F, Tiede S, Christofori G. Breast cancer as an example of tumour heterogeneity and tumour cell plasticity during malignant progression. *Br J Cancer.* 2021;125(2):164–75.
- Kavousi M, Chavoshi M. Effect of coated carbon nanotubes with Chitosan and cover of flaxseed in the induction of MDA-MB-231 apoptosis by analyzing the expression of Bax and Bcl-2. *Meta Gene.* 2020;26:100807.
- Ebadi M, et al. Investigation of the apoptotic and antimetastatic effects of Nano-Niosomes containing the plant extract *anabasis setifera* on HeLa: in vitro cervical Cancer study. *Chem Biodivers.* 2024;0:e202402599.
- Raj S, et al. Specific targeting cancer cells with nanoparticles and drug delivery in cancer therapy. *Seminars in cancer biology.* Elsevier; 2021.
- Jin C, et al. Application of nanotechnology in cancer diagnosis and therapy-a mini-review. *Int J Med Sci.* 2020;17(18):2964.
- Pinto CS, Dos Santos EP, Mansur CRE. Niosomes as nano-delivery systems in the pharmaceutical field. *Crit Reviews™ Therapeutic Drug Carrier Syst.* 2016;33(2).
- Ge X, et al. Advances of non-ionic surfactant vesicles (niosomes) and their application in drug delivery. *Pharmaceutics.* 2019;11(2):55.
- Pandey P et al. Advancement and characteristics of Non-Ionic surfactant vesicles (Niosome) and their application for analgesics. *Int J Pharm Invest.* 2024;14(3).
- Moammeri A et al. Current advances in niosomes applications for drug delivery and cancer treatment. *Mater Today Bio.* 2023. 100837.
- Hassan SH, et al. Alpha solanine: A novel natural bioactive molecule with anticancer effects in multiple human malignancies. *Nutr Cancer.* 2021;73(9):1541–52.
- Huang M, Lu J-J, Ding J. Natural products in cancer therapy: past, present and future. *Nat Prod Bioprospecting.* 2021;11(1):5–13.
- Morillo M, et al. Natural and synthetic derivatives of the steroidal glycoalkaloids of *Solanum* genus and biological activity. *Natural Products Chemistry & Research;* 2020.
- Zou T, et al. Alpha-solanine anti-tumor effects in non-small cell lung cancer through regulating the energy metabolism pathway. *Recent Pat Anti-cancer Drug Discov.* 2022;17(4):396–409.
- Nandi S, et al. Updated aspects of alpha-Solanine as a potential anti-cancer agent: mechanistic insights and future directions. *Food Sci Nutr.* 2024;12(10):7088–107.
- Ni X, et al. Anti-cancer effect of α -solanine by down-regulating S100P expression in colorectal cancer cells. *Recent Pat Anti-cancer Drug Discov.* 2018;13(2):240–7.
- Kavousi M, et al. Solanum pseudo-capsicum effects on Bax and Bcl-2 gene expression and apoptosis in MCF-7 cell line. *Genetika-Belgrade.* 2023;55(2):523–36. <https://doi.org/10.2298/GENSR2302523K>.
- Mirzaei-Parsa MJ, et al. Preparation, characterization, and evaluation of the anticancer activity of artemether-loaded nano-niosomes against breast cancer. *Breast Cancer.* 2020;27:243–51.
- Ahmadi S, et al. In vitro development of controlled-release nanoniosomes for improved delivery and anticancer activity of letrozole for breast cancer treatment. *Int J Nanomed.* 2022;17:6233.
- Barani M, et al. In vitro and in vivo anticancer effect of pH-responsive paclitaxel-loaded niosomes. *J Mater Science: Mater Med.* 2021;32:1–13.
- Rahdar A, et al. Effect of Tocopherol on the properties of pluronic F127 microemulsions: Physico-chemical characterization and in vivo toxicity. *J Mol Liq.* 2019;277:624–30.
- Homaei S, et al. Investigating the apoptotic and antimetastatic effect of daphnetin-containing nano niosomes on MCF-7 cells. *Adv Cancer Biology–Metastasis.* 2025. <https://doi.org/10.1016/j.adcanc.2025.100139>.
- Pourmoghadasian B, et al. Nanosized paclitaxel-loaded niosomes: formulation, in vitro cytotoxicity, and apoptosis gene expression in breast cancer cell lines. *Mol Biol Rep.* 2022;49(5):3597–608.
- Bojar Doulaby D, et al. Effect of Dioscorea extract on Bax and Bcl-2 gene expression in MCF-7 and HFF cell lines. *Egypt J Med Hum Genet.* 2023;24:70. <https://doi.org/10.1186/s43042-023-00450-w>.
- Agarwal S, et al. Formulation, characterization and evaluation of Morusin loaded niosomes for potentiation of anticancer therapy. *RSC Adv.* 2018;8(57):32621–36.
- Barani M, et al. Lawsone-loaded niosome and its antitumor activity in MCF-7 breast Cancer cell line: a Nano-herbal treatment for Cancer. *DARU J Pharm Sci.* 2018;26:11–7.
- You L, et al. Synthesis of multifunctional Fe₃O₄@ PLGA-PEG nano-niosomes as a targeting carrier for treatment of cervical cancer. *Mater Sci Engineering: C.* 2019;94:291–302.
- Askarizadeh A, et al. Doxorubicin-loaded liposomes surface engineered with the matrix metalloproteinase-2 cleavable polyethylene glycol conjugate for cancer therapy. *Cancer Nanotechnol.* 2023;14(1):18.
- Ukwubile CA, Ikpefan EO, Famurewa AC. Role of Chitosan-Loaded solanine glycoalkaloid from *Solanum scabrum* mill. Leaf extract as Anti-Inflammatory and in vitro anticancer agents. *Turkish J Pharm Sci.* 2023;20(4):240.
- Ling B, et al. Probing the antitumor mechanism of *Solanum nigrum* L. aqueous extract against human breast cancer MCF7 cells. *Bioengineering.* 2019;6(4):112.
- Muñoz-Pinedo C. Signaling pathway that regulate life and cell death. *Self Nonself.* 2012; 124.
- Green DR. The mitochondrial pathway of apoptosis part II: the BCL-2 protein family. *Cold Spring Harb Perspect Biol.* 2022;14(6):a041046.
- Qian ZR, et al. Tumor-specific downregulation and methylation of the CDH13 (H-cadherin) and CDH1 (E-cadherin) genes correlate with aggressiveness of human pituitary adenomas. *Mod Pathol.* 2007;20(12):1269–77.

38. Banerjee S et al. CDH1 gene as biomarker towards breast cancer prediction. *J Biomol Struct Dynamics*. 2024. 1–14.
39. Song Z, et al. The role of MMP-2 and MMP-9 in the metastasis and development of hypopharyngeal carcinoma. *Braz J Otorhinolaryngol*. 2021;87:521–8.
40. Lu M-K, et al. α -Solanine inhibits human melanoma cell migration and invasion by reducing matrix metalloproteinase-2/9 activities. *Biol Pharm Bull*. 2010;33(10):1685–91.
41. Shen K-H, et al. α -Solanine inhibits invasion of human prostate cancer cell by suppressing epithelial-mesenchymal transition and MMPs expression. *Molecules*. 2014;19(8):11896–914.

Publisher's note

Springer Nature remains neutral with regard to jurisdictional claims in published maps and institutional affiliations.